XII International Conference on Computational Plasticity. Fundamentals and Applications
COMPLAS XII
E. Oñate, D.R.J. Owen, D. Peric and B. Suárez (Eds)

MODELING AND EXPERIMENTAL INVESTIGATIONS OF THE STRESS-SOFTENING BEHAVIOR OF SOFT COLLAGENOUS TISSUES

THOMAS SCHMIDT*, DANIEL BALZANI*, ANDREAS J. SCHRIEFL† AND GERHARD A. HOLZAPFEL†,**

* Institute of Mechanics, University of Duisburg-Essen, Faculty for Engineering Sciences,
Department of Civil Engineering, Universitätsstr. 15, 45141 Essen, Germany
e-mail: t.schmidt@uni-due.de, daniel.balzani@uni-due.de
website: www.uni-due.de/mechanika/index_englisch.php

†Graz University of Technology, Institute of Biomechanics, Center of Biomedical Engineering
Kronesgasse 5-I, 8010 Graz, Austria
e-mail: schriefl@tugraz.at, holzapfel@tugraz.at — website: www.biomech.tugraz.at

**Royal Institute of Technology, Department of Solid Mechanics,
School of Engineering Sciences, Teknikringen 8d, 100 44 Stockholm, Sweden

Key words: Collagen, Artery, Microstructure, Biomechanics, Constitutive Modeling

Abstract. This paper deals with the formulation of a micro-mechanically based damage model for soft collagenous tissues. The model is motivated by (i) a sliding filament model proposed in the literature [1] and (ii) by experimental observations from electron microscopy (EM) images of human abdominal aorta specimens, see [2]. Specifically, we derive a continuum damage model that takes into account statistically distributed proteoglycan (PG) bridges. The damage model is embedded into the constitutive framework proposed by Balzani *et al.* [3] and adjusted to cyclic uniaxial tension tests of a human carotid artery. Furthermore, the resulting damage distribution of the model after a circumferential overstretch of a simplified arterial section is analyzed in a finite element calculation.

1 INTRODUCTION

The softening behavior of soft collagenous tissues is relevant when the tissue is subjected to supra-physiological loading situations. They occur, for example, during clinical interventions such as balloon angioplasty, where an atherosclerotic artery is circumferentially overstretched. Thereby, a softening of the tissue is observed, which is one of the

main contributors to the success of the treatment since it leads to an increase of the arterial lumen in the physiological loading domain. The softening is believed to result from microscopic tissue 'damage'. Thus, to model this phenomenon, the framework of continuum damage mechanics, cf. Simo [4], is usually applied. In addition, phenomenological approaches following the pseudo-elasticity concept (see Ogden & Roxburg [5]) have been applied to soft collagenous tissues, see, for example, Weisbecker *et al.* [6]. An important aspect of a model is to account for the tissue's anisotropy, which results from the alignment of collagen fibers, cf. [7], [8]. A practical approach, that avoids the introduction of tensorial damage quantities, uses scalar-valued variables, see [9]. To reflect remanent strains, that can be observed in soft collagenous tissues after overstretching, Gasser & Holzapfel [10] modeled remaining deformations of the fibers. Whereas, in the latter publication finite plasticity was considered, Ehret & Itskov [11] described remanent fiber deformation in a continuum damage mechanics framework. Balzani *et al.* [3] proposed a construction principle for damage models allowing the desciption of remanent strains and furthermore ensuring polyconvexity in the undamaged (physiological) regime. Other authors such as Natali *et al.* [12] or Calvo *et al.* [13] considered damage to occur in the collagen fibers as well as in the matrix material.

The above mentioned models are of phenomenological character. As a first micromechanical approach Rodríguez *et al.* [14] traced damage back to the subsequent rupture of collagen fibers and considered their waviness to be stochastically distributed. Gasser [15] formulated a phenomenological damage model motivated by the loss of interfibrillar proteoglycan (PG) bridges. This idea is based on a sliding filament model proposed by Scott [1] stating that the interconnecting PG bridges between collagen fibrils store strains reversibly as long as a certain threshold is not exceeded.

In the present contribution, we derive a micromechanical approach for damage, which is also motivated by [1]. Therefore, in a first step, we experimentally investigate human arterial tissue from abdominal aortas on the fibrillar level by means of electron microscopy (EM), for details see [2]. From these EM images it can be deduced, that dispersed microscopic quantities may be indeed taken into account. Thus, a damage model is formulated assuming a statistical distribution of proteoglycan orientation and it is incorporated into the constitutive framework [3]. The model parameters are adjusted to cyclic uniaxial tension data of human carotid artery specimens, and used in a numerical example within a finite element framework. Remarks concerning the algorithmic implementation of the model as well as alternative approaches for the incorporation of statistical distributions and related adjustment results are provided in [16].

2 EXPERIMENTAL ANALYSIS

Due to the aforementioned assumption that damage in collagenous tissues takes place at the fibril level, microstructural experiments were carried out at Graz University of Technology. Thereby, human arterial specimens of the abdominal aorta were considered

and investigated via electron microscopy (EM) imaging to visualize microstructural tissue components. Therefore, a staining with Cupromeronic Blue (CB) was performed according to [17]. For the EM imaging ultra-thin sections (200-300 nm) were taken by means of a microtome equipped with a diamond knife. The resulting images show collagen fibrils and PGs, see Fig. 1(a). Even though we only observe two-dimensional (2D) projections on the EM imaging plane of originally three-dimensionally (3D) oriented PGs in space, it can be seen that the PGs are not aligned in a unique direction between the collagen fibrils, but they are rather dispersed. Furthermore, we investigated the distances between collagen fibrils with the help of a custom programmed plugin for the ImageJ software (U.S. National Institutes of Health, MD, USA), that identifies the cross-sections of collagen fibrils and the interfibrillar distances (see [2] for more details). Due to their high variability, the number of soft tissue samples was too small to serve as a solid data base for quantifying statistical distributions of the investigated quantities. However, the obtained results show that it is reasonable to take into account the distributed microscopical parameters for the numerical modeling of soft collagenous tissues.

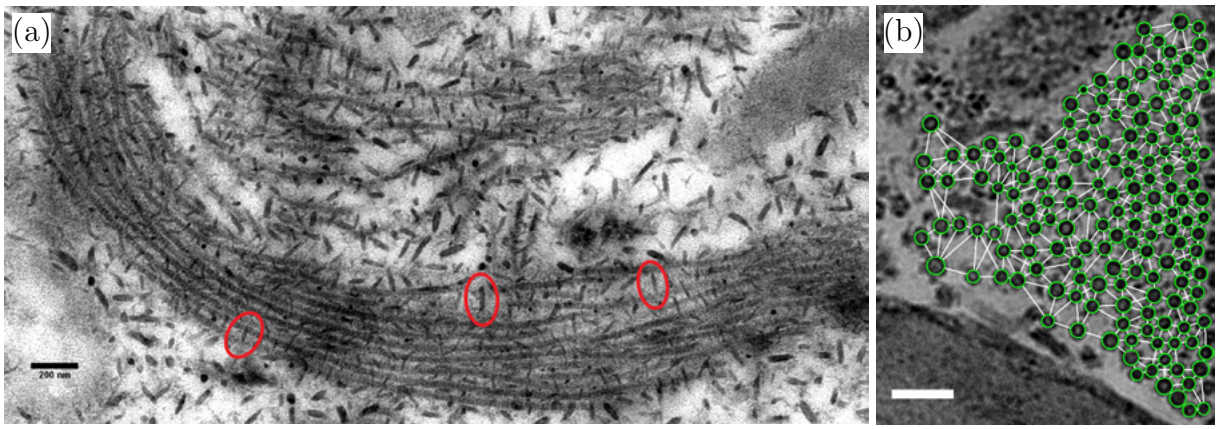

Figure 1: Transmission electron microscopy images: (a) collagen fibrils and proteoglycans (PGs) (three are highlighted by red circles). Scale bar: 200 nm; (b) highlighted cross-sectioned collagen fibrils that were identified (green circles) by the custom programmed ImageJ plugin. Scale bar: 200 nm.

3 MATHEMATICAL MODEL

3.1 CONTINUUM MECHANICAL MODELING

According to standard continuum mechanics, we consider the deformation gradient $\boldsymbol{F}$ with $J := \det \boldsymbol{F} > 0$ and the right Cauchy-Green tensor $\boldsymbol{C} := \boldsymbol{F}^T \boldsymbol{F}$. For hyperelastic materials a strain-energy function $\Psi := \Psi(\boldsymbol{C})$ is defined per unit reference volume, and the second Piola-Kirchhoff stress tensor can be obtained by $\boldsymbol{S} = 2\partial_{\boldsymbol{C}}\Psi$. The physical Cauchy

stresses are given by a push-forward operation as $\boldsymbol{\sigma} = J^{-1}\boldsymbol{F}\boldsymbol{S}\boldsymbol{F}^T$. When describing fiber-reinforced materials, the dependence of the deformation on the fiber directions $\boldsymbol{A}_{(a)}$ is accounted for by the incorporation of structural tensors $\boldsymbol{M}_{(a)} := \boldsymbol{A}_{(a)} \otimes \boldsymbol{A}_{(a)}$, with $a = 1, \ldots, n_\mathrm{a}$, for a given number of fiber families n_a. Therefore, the invariants $I_1 := \mathrm{tr}\boldsymbol{C}$, $I_2 := \mathrm{tr}[\mathrm{Cof}\boldsymbol{C}]$ with $\mathrm{Cof}[\boldsymbol{C}] = \det[\boldsymbol{C}]\boldsymbol{C}^{-1}$, and $I_3 := \det\boldsymbol{C}$ of the right Cauchy-Green tensor, and the mixed invariants $J_4^{(a)} := \mathrm{tr}[\boldsymbol{C}\boldsymbol{M}_{(a)}]$ and $J_5^{(a)} := \mathrm{tr}[\boldsymbol{C}^2\boldsymbol{M}_{(a)}]$ are taken into account for the formulation of the strain energy. Instead of $J_5^{(a)}$, which is not polyconvex, the alternative polyconvex functions

$$\begin{aligned} K_1^{(a)} &:= \mathrm{tr}[\mathrm{Cof}\boldsymbol{C}\boldsymbol{M}_{(a)}] = J_5^{(a)} - I_1 J_4^{(a)} + I_2, \\ K_2^{(a)} &:= \mathrm{tr}[\boldsymbol{C}(\boldsymbol{I} - \boldsymbol{M}_{(a)})] = I_1 - J_4^{(a)}, \\ K_3^{(a)} &:= \mathrm{tr}[\mathrm{Cof}\boldsymbol{C}(\boldsymbol{I} - \boldsymbol{M}_{(a)})] = I_1 J_4^{(a)} - J_5^{(a)} \end{aligned} \tag{1}$$

can be used, see Schröder & Neff [18]. Soft collagenous tissues are often described by a decomposition of the total strain energy according to

$$\Psi = \Psi^{\mathrm{pen}}(\det\boldsymbol{C}) + \Psi^{\mathrm{iso}}(\boldsymbol{C}) + \sum_{a=1}^{n_a} \Psi^{\mathrm{ti}}_{(a)}(\boldsymbol{C}, \boldsymbol{M}_{(a)}). \tag{2}$$

Herein, the term Ψ^{pen} penalizes deviations from isochoric deformations. For the contribution of the isotropic matrix material we use here $\Psi^{\mathrm{iso}} = c_1(I_1/I_3^{1/3} - 3)$ with the stress-like parameter c_1. A number of $n_\mathrm{a} = 2$ transversely-isotropic energies $\Psi^{\mathrm{ti}}_{(a)}$ is superimposed to account for two fiber families as observed in arterial tissues. For the formulation of $\Psi^{\mathrm{ti}}_{(a)}$ the constitutive framework, as proposed in Balzani *et al.* [3], is used. This enables us to describe remanent strains in the physiological loading domain after supra-physiological loadings. Furthermore, polyconvexity is ensured in the physiological (undamaged) domain. According to the framework, a one-dimensional damage variable $D_{(a)} \in [0, 1]$ is incorporated into an internal function as

$$\Psi^{\mathrm{ti}}_{(a)} := m[P_{(a)}(\boldsymbol{C}, D_{(a)})] \qquad \text{with} \qquad P_{(a)} = (1 - D_{(a)})\Psi^{\mathrm{ti},0}_{(a)} - c. \tag{3}$$

Herein, c equals the value of the effective transversely isotropic function $\Psi^{\mathrm{ti},0}_{(a)}$ in the reference configuration. Polyconvex functions such as, for example, J_4 or K_3, can be used as the effective (undamaged) function $\Psi^{\mathrm{ti},0}_{(a)}$. The internal function $P_{(a)}$ is embedded in an external function $m[P(X)]$, which must be convex and monotonically increasing. The second Piola-Kirchhoff stress tensor $\boldsymbol{S}$ resulting from (2) reads

$$\boldsymbol{S} = 2\frac{\partial\Psi}{\partial\boldsymbol{C}} = \boldsymbol{S}^{\mathrm{pen}} + \boldsymbol{S}^{\mathrm{iso}} + \sum_{a=1}^{n_a} \boldsymbol{S}^{\mathrm{ti}}_{(a)}, \qquad \text{with} \qquad \boldsymbol{S}^{\mathrm{pen}} = 2\frac{\partial\Psi^{\mathrm{pen}}}{\partial\boldsymbol{C}}, \quad \boldsymbol{S}^{\mathrm{iso}} = 2\frac{\partial\Psi^{\mathrm{iso}}}{\partial\boldsymbol{C}}, \tag{4}$$

and the transversely isotropic part is

$$\boldsymbol{S}^{\mathrm{ti}}_{(a)} = (1 - D_{(a)})\boldsymbol{S}^{\mathrm{ti},0}_{(a)} \qquad \text{with} \qquad \boldsymbol{S}^{\mathrm{ti},0}_{(a)} = 2\partial_P m\frac{\partial\Psi^{\mathrm{ti},0}_{(a)}}{\partial\boldsymbol{C}}. \tag{5}$$

With the above described constitutive framework, the challenge that still arises is a suitable definition for $\Psi^{\mathrm{ti},0}_{(a)}$ and the damage variable $D_{(a)}$. While for the effective function characterizing the physiological behavior some micromechanically motivated formulations are provided in the literature, see, for example, [19], [20], there are a few damage functions available that directly take into account the microscopic findings.

3.2 MICROMECHANICALLY-BASED DAMAGE FUNCTION

In order to derive a micromechanically-based damage function we follow the idea of a sliding filament model, as proposed by Scott *et al.* [1]. The model states that PG bridges store reversible strains in a certain domain, which is due to their composition of two neighboring anionic glycosaminoglycan (AGAG) chains. In the case of an applied stress the AGAG chains can bond differently and thus enable sliding of collagen fibrils relatively to each other. Since the latter process is only possible in a certain domain, there exists some threshold value for a sustainable PG stretch, which we denote here as $\lambda^{\mathrm{sust}}_{\mathrm{pg}}$. In order to identify a domain of PG bridges, where this threshold is exceeded, the fibril-proteoglycan microstructure in Fig. 2(a) is considered as a unit-cell. Therein, we regard two half collagen fibrils and interconnecting PG bridges. The unit-cell undergoes a deformation due to a fiber stretch $\lambda_{\mathrm{fib}} = \sqrt{J_4}$, such that the initial distance d_0 between collagen fibrils changes to d, and the PG orientation α changes. Since we assume here the tissue to be incompressible the transverse stretch to the fiber direction is $1/\sqrt{\lambda_{\mathrm{fib}}}$ and, therefore, the distance of collagen fibrils in the deformed configuration is given by

$$d = \frac{d_0}{\sqrt{\lambda_{\mathrm{fib}}}}. \tag{6}$$

With trigonometric arguments the following expression for the PG stretch can be derived as the ratio of the undeformed ($L_{\mathrm{pg},0}$) and the deformed (L_{pg}) lengths, i.e.

$$\lambda_{\mathrm{pg}} = \frac{L_{\mathrm{pg}}}{L_{\mathrm{pg},0}} = \sqrt{\left[\cos\alpha - L(\lambda_{\mathrm{fib}} - 1)\sin\alpha\right]^2 + \frac{\sin^2\alpha}{\lambda_{\mathrm{fib}}}}. \tag{7}$$

Herein, we introduced the dimensionless internal length parameter $L = (L_{\mathrm{cf}} - L_{\mathrm{ov}})/d_0$, with the initial length L_{cf} of collagen fibrils, their initial overlap L_{ov} and distance d_0 to each other.

Motivated by our experimental findings, see Fig. 1(a), we assume here the angle α to be statistically distributed. With the help of the parameter $\lambda^{\mathrm{sust}}_{\mathrm{pg}}$ a regime of failed PG bridges is given by $\lambda_{\mathrm{pg}} - \lambda^{\mathrm{sust}}_{\mathrm{pg}} \geq 0$. Thus, a lower and an upper regime bound α_l and α_u can be evaluated as solutions of

$$\lambda_{\mathrm{pg}} - \lambda^{\mathrm{sust}}_{\mathrm{pg}} = 0, \tag{8}$$

see Fig. 2(b). The damage variable D is defined as the fraction of failing PG bridges.

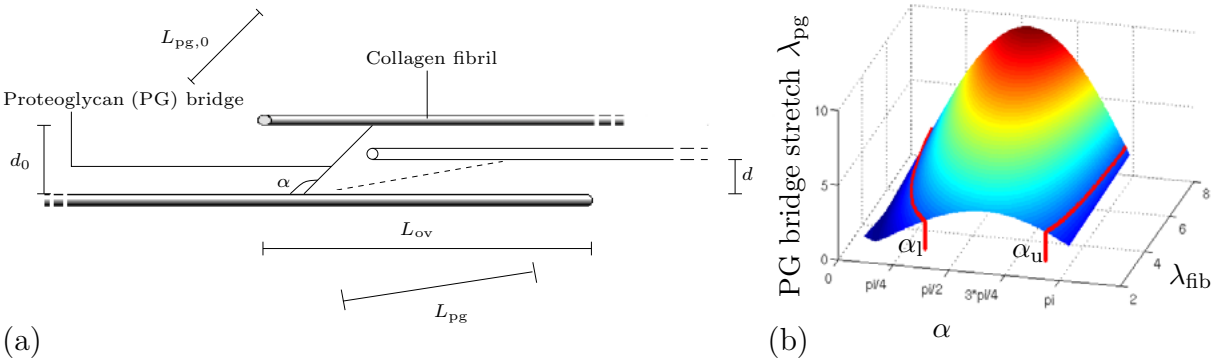

Figure 2: (a) Geometrical quantities defining the fibril-proteoglycan microstructure in the reference and current configurations; (b) lower and upper bounds (α_l, α_u) for a domain of ruptured PG bridges under consideration of a statistically distributed PG orientation α; pictures are taken from SCHMIDT *et al.* [16].

Therefore, it is evaluated as the integral of the respective probability density function (PDF) ϑ of α over α_{l} and α_{u}, i.e.

$$D(\lambda_{\mathrm{fib}}) = \int_{\alpha_{\mathrm{l}}(\lambda_{\mathrm{fib}})}^{\alpha_{\mathrm{u}}(\lambda_{\mathrm{fib}})} \vartheta(\alpha)\mathrm{d}\alpha = \hat{\vartheta}(\alpha_{\mathrm{u}}) - \hat{\vartheta}(\alpha_{\mathrm{l}}) \quad \text{with} \quad \int_{\alpha} \vartheta(\alpha)\mathrm{d}\alpha = 1. \tag{9}$$

According to the above definition $0 \leq D \leq 1$ holds, while $\hat{\vartheta}$ denotes the cumulative distribution function (CDF). Due to the limitation $0 < \alpha < \pi$, see Fig. 2(a), a beta distribution is taken with the open interval $0 < \bar{\alpha} < 1$ and $\bar{\alpha} = \alpha/\pi$. Thus, the CDF is given by

$$\hat{\vartheta}_{\mathrm{beta}}(\bar{\alpha}) = \frac{1}{B(a,b)} \int_0^{\bar{\alpha}} \tilde{\alpha}^{a-1}(1-\tilde{\alpha})^{b-1}\mathrm{d}\tilde{\alpha} \quad \text{with} \quad 0 < \bar{\alpha} < 1, \tag{10}$$

and a, b denote parameters of the beta distribution, and B denotes the beta function.

4 ADJUSTMENT TO EXPERIMENTAL DATA

In this section the derived micromechanical damage function is combined with two different transversely-isotropic strain-energy functions, as introduced by BALZANI *et al.* [20], i.e.

$$\Psi^{\mathrm{ti}}_{\mathrm{BNSH_e}} = \frac{k_1}{2k_2}\left\{\exp\left[k_2\left\langle(1-D_{(a)})K_3^{(a)} - 2\right\rangle^2\right] - 1\right\}, \tag{11}$$

$$\Psi^{\mathrm{ti}}_{\mathrm{BNSH_p}} = \alpha_1\langle(1-D_{(a)})K_3^{(a)} - 2\rangle^{\alpha_2}, \tag{12}$$

Table 1: Material parameters and error measure $\overline{r}$ for the models $\Psi_{\mathrm{BNSH_e}}$ and $\Psi_{\mathrm{BNSH_p}}$ for the media of a human carotid artery under consideration of a beta distributed PG orientation; see relation (2) with the use of (11) and the microscopical parameters according to Section 3.2, cf. [16].

	c_1 [kPa]	$k_1 \vert \alpha_1$ [kPa]	k_2 [-]	α_2 [-]	β_f [°]	$\lambda_\mathrm{pg}^\mathrm{sust}$ [-]	L [-]	a [-]	b [-]	$\overline{r}$ [-]
$\Psi_{\mathrm{BNSH_e}}$	9.58	894.38	87.0	–	39.40	1.0158	3.8	9.8	18.9	0.067
$\Psi_{\mathrm{BNSH_p}}$	9.75	1003.8	–	2.06	39.39	1.0068	4.7	5.4	13.7	0.073

with the stress-like parameters $k_1 > 0$ and $\alpha_1 > 0$, and the dimensionless parameters $k_2 > 0$ and $\alpha_2 > 0$. The total strain-energy functions are denoted accordingly as $\Psi_{\mathrm{BNSH_e}}$ and $\Psi_{\mathrm{BNSH_p}}$. The respective material response is adjusted to uniaxial cyclic tension data of a human carotid artery, as in Balzani *et al.* [3]. Therein, the following least-square function is minimized

$$\bar{r}(\boldsymbol{\alpha}) = \sum_{\mathrm{k}=1}^{n_\mathrm{exp}} \sqrt{\frac{1}{n_\mathrm{mp}} \sum_{i=1}^{n_\mathrm{cyc}} \sum_{j=1}^{n_{\mathrm{mp},i}} r(\boldsymbol{\alpha})}, \quad r(\boldsymbol{\alpha}) = \left(\frac{\sigma^\mathrm{exp}(\lambda^{(i,j)}) - \sigma^\mathrm{comp}(\lambda^{(i,j)}, \boldsymbol{\alpha})}{\max\limits_j \left(\sigma^\mathrm{exp}\right)} \right)^2 \tag{13}$$

with respect to the vector $\boldsymbol{\alpha}$ of material parameters. The stretch in the tension direction is denoted by λ. The deviation between the experimental stress σ^exp and the computed stress σ^comp is normalized by the maximum experimental stress in the respective extension cycle i. The squares of these expressions are summed up over n_cyc extension cycles with $n_{\mathrm{mp},i}$ measured points j each. The overall sum is divided by the overall number of measured points n_mp and the square root is computed. The resulting error measures are summarized for $n_\mathrm{exp} = 2$ experiments, namely a cyclic uniaxial tension test in the circumferential direction and one in the axial direction of the artery. Note, that $\boldsymbol{\alpha}$ also contains the angle β_f between the fiber direction and the circumferential direction of the artery as well as the microscopical parameters from Section 3.2 due to the aforementioned lack of a data basis.

Within the optimization, the stretches in the transverse directions are determined by an iterative procedure under the assumption of incompressibility such that a uniaxial stress state is obtained. The resulting stress response with the adjusted material parameters is given in Fig. 3. As can be seen, a good correlation with the experimental data can be obtained with both transversely-isotropic functions, whereas $\Psi_{\mathrm{BNSH_e}}$ performs slightly better.

5 NUMERICAL EXAMPLE

In this section the applicability of the proposed damage model in a finite element calculation is shown. Therefore, the circumferential overstretch of a simplified section of an

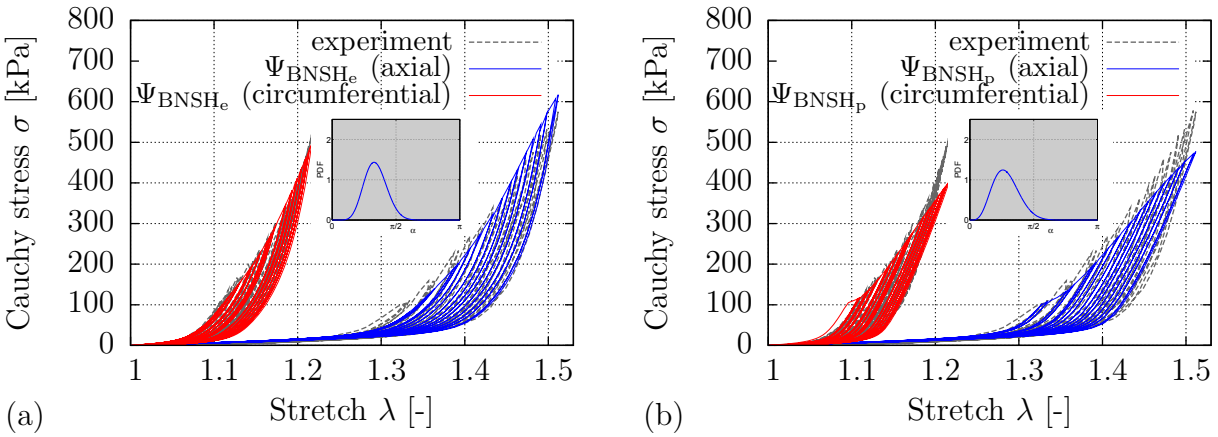

Figure 3: Cyclic uniaxial tension tests of the media of a human carotid artery: (a) experimental data and results of the constitutive model $\Psi_{\mathrm{BNSH_e}}$; (b) experimental data and results of the constitutive model $\Psi_{\mathrm{BNSH_p}}$, cf. [16]. The PG orientation is assumed to be beta distributed. The associated material parmeters are given in Table 1.

atherosclerotic artery is numerically simulated. Five different tissue layers are considered: fibrous cap, lipid pool, (diseased) fibrotic media, (non-diseased) media, and adventitia, see Fig. 4(a). The model is discretized with 7963 quadratic tetrahedral elements. For the non-diseased media the model $\Psi_{\mathrm{BNSH_p}}$ with the obtained parameters from Table 1 is used. For the other layers, except for the lipid pool, the same adjustment routine, as described in the previous section, was performed (see [3] for the specific experiments). Due to missing experimental data in the supra-physiological domain for the fibrous cap and the fibrotic media, only the hyperelastic parameters of these layers were adjusted to experimental data and the same damage parameters as for the media were taken. Specifically, the model $\Psi_{\mathrm{BNSH_e}}$ is used for the fibrotic media and the model $\Psi_{\mathrm{BNSH_p}}$ is applied to the fibrous cap and the adventitia. The lipid pool is considered to be butter-like and incompressible, and is, therefore, modeled as a neo-Hookean material with a significantly lower stiffness than the other components. Damage is not assumed to occur in the lipid pool. Table 2 summarizes all material parameters and the obtained error measure $\overline{r}$ from the adjustment procedure.

The penalty term $\Psi^{\mathrm{pen}} = \epsilon_1 \left(I_3^{\epsilon_2} + I_3^{-\epsilon_2} - 2\right)$ is used to control the volumetric behavior. For the adventitia, the non-diseased media, the fibrotic media and the fibrous cap $\epsilon_1 = 50.0\,\mathrm{kPa}$ and $\epsilon_2 = 20.0$ were set, whereas for the lipid pool we used $\epsilon_1 = 20.0\,\mathrm{kPa}$ and $\epsilon_2 = 10.0$. These penalty parameters ensured that the quasi-incompressibility constraint $\det \boldsymbol{F} = 1 \pm 1\%$ was fulfilled at any integration point during the computation. An internal pressure is applied to the arterial lumen. A first loading branch increases up to 24.0 kPa ($\hat{=}$180.0 mmHg) which was regarded here as the very upper limit of the physiological blood pressure. Furthermore, during this first loading branch, an axial strain of 2% is applied in order to incorporate residual axial stretches. This was neglected in the circumferential direction since the associated circumferential stresses are assumed to be

Table 2: Hyperelastic and damage parameters of four tissue components. Parameters for the non-diseased media are taken from Table 1, cf. [16].

	c_1 [kPa]	$k_1\|\alpha_1$ [kPa]	$k_2\|\alpha_2$ [-]	β_f [°]	$\lambda_\mathrm{pg}^\mathrm{sust}$ [-]	L [-]	a [-]	b [-]	$\overline{r}$ [-]
Adventitia	5.7	8159.4	3.5	45.59	1.1235	9.746	8.11	24.33	0.1213
Fibrotic media	20.9	479.36	293.3	25.18	1.0068	4.711	5.42	13.67	0.0177
Fibrous cap	27.3	1222.4	2.0	50.93	1.0068	4.711	5.42	13.67	0.0367
Lipid pool	50.0	–	–	–	–	–	–	–	–

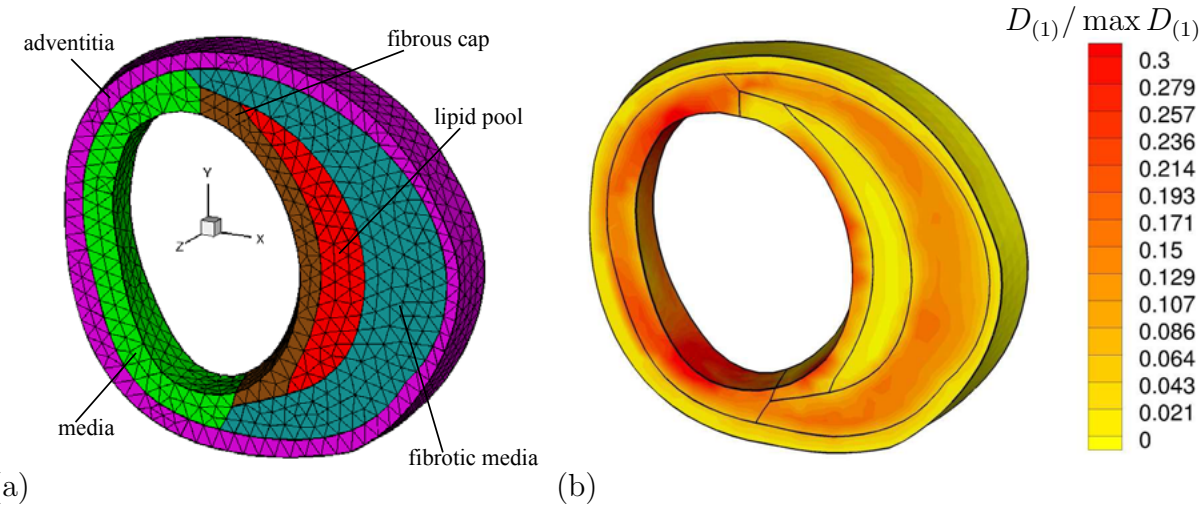

(a) (b)

Figure 4: (a) Three-dimensional finite element model of a thin section of a diseased artery with five different tissue layers discretized with 7963 quadratic tetrahedral elements; (b) distribution of the normalized damage variable $D_{(1)}/\max D_{(1)}$ of the first fiber family in the arterial section at an internal pressure of 82 kPa; cf. [16].

significantly lower compared to the ones occurring due to the overstretch. In a further loading branch the internal pressure increases to 82.0 kPa ($\hat{=}$615.0 mmHg) yielding an overstretch of the artery. In Fig. 4(b) the normalized damage variable $D_{(1)}/\max D_{(1)}$ with $\max D_{(1)} = 0.108$ is depicted at $p = 82.0$ kPa. High damage values due to the overstretch can be observed in the media and the fibrous cap, whereas rather low damage occurs in the adventitia. These results are compatible with the ones reported in Balzani *et al.* [3].

6 CONCLUSIONS

In this contribution a micromechanical approach for damage in soft collagenous tissues was derived. The approach considers statistically distributed orientations of proteoglycan

bridges and a subsequent loss of those due to overstretch. A comparison with cyclic experimental data of a human carotid artery in the supra-physiological loading domain showed good agreement such that we may conclude that a subsequent loss of proteoglycan bridges is an important contributor to softening of collagenous tissues. Furthermore, with the help of the derived model, the circumferential overstretch of a simplified atherosclerotic artery, as it occurs during balloon angioplasty, was numerically simulated. A pronounced damage was observed in the healthy media and in the fibrous cap after that overstretch.

ACKNOWLEDGEMENTS

The authors greatly appreciate the German Science Foundation (DFG) and the Austrian Science Fund (FWF) for the financial support under the research grants BA 2823/5-1 and I 503-B11, respectively. Further thanks go to Gerhard Sommer at Graz University of Technology, who carried out the cyclic tension tests in the supra-physiological loading domain.

REFERENCES

[1] Scott, J.E. Elasticity in extracellular matrix shape modules of tendon, cartilage, etc. A sliding proteoglycan-filament model. *Journal of Physiology*, 553:335–343, 2003.

[2] Schriefl, A.J., Schmidt, T., Balzani, D. and Holzapfel, G.A. Determination of mechanical and microstructural tissue quantities for modeling damage in arterial tissues. *Dreiländertagung der Deutschen, Schweizerischen und Österreichischen Gesellschaft für Biomedizinische Technik*, 2013.

[3] Balzani, D., Brinkhues, S. and Holzapfel, G.A. Constitutive framework for the modeling of damage in collagenous soft tissues with application to arterial walls. *Comput. Meth. Appl. Mech. Eng.*, 213–216:139–151, 2012.

[4] Simo, J.C. On a fully three-dimensional finite-strain viscoelastic damage model: formulation and computational aspects. *Comput. Meth. Appl. Mech. Eng.*, 60:153–173, 1987.

[5] Ogden, R.W. and Roxburg, D.G. An energy-based model of the Mullins effect. In A. Dorfmann and A. Muhr, editors, *Proceedings of the First European Conference on Constitutive Models*, pages 23–28. A. A. Balkema, Rotterdam, Brookfield, 1999.

[6] Weisbecker, H., Pierce, D.M., Regitnig, P. and Holzapfel, G.A. Layer-specific damage experiments and modeling of human thoracic and abdominal aortas with non-atherosclerotic intimal thickening. *J. Mech. Behav. Biomed.*, 12:93–106, 2012.

[7] Schriefl, A.J., Reinisch, A.J., Sankaran, S., Pierce, D.M. and Holzapfel, G.A. Quantitative assessment of collagen fiber orientations from 2D images of soft biological tissues. *J. R. Soc. Interface*, 9:3081–3093, 2012.

[8] Schriefl, A.J., Wolinski, H., Regitnig, P., Kohlwein, S.D. and Holzapfel, G.A. An automated approach for 3D quantification of fibrillar structures in optically cleared soft biological tissues. *J. R. Soc. Interface*, 10:20120760, 2013.

[9] Balzani, D., Schröder, J., Gross, D. Simulation of discontinuous damage incorporating residual stresses in circumferentially overstretched atherosclerotic arteries. *Acta Biomater.*, 2: 609–618, 2006

[10] Gasser, T.C. and Holzapfel, G.A. Finite element modeling of balloon angioplasty by considering overstretch of remnant non-diseased tissues in lesions. *Comput. Mech.*, 40:47–60, 2007.

[11] Ehret, A. and Itskov, M. Modeling of anisotropic softening phenomena: Application to soft biological tissues. *Int. J. Plasticity*, 25:901–919, 2007.

[12] Natali, A.N., Pavan, P.G., Carniel, E.L. and Dorow, C. A transversally isotropic elasto-damage constitutive model for the periodontal ligament. *Comput. Method. Biomec.*, 6:329–336, 2003.

[13] B. Calvo, E. Peña, M.A. Martínez, and M.A. Doblaré. An uncoupled directional damage model for fibered biological soft tissues. *Int. J. Numer. Meth. Eng.*, 69:2036–2057, 2007.

[14] Rodríguez, J.F., Cacho, F., Bea, J.A. and Doblaré, M. A stochastic-structurally based three dimensional finite-strain damage model for fibrous soft tissue. *J. Mech. Phys. Solids*, 54:864–886, 2006.

[15] Gasser, T.C. An irreversible constitutive model for fibrous soft biological tissue: A 3-D microfiber approach with demonstrative application to abdominal aortic aneurysms. *Acta Biomater.*, 7:2457–2466, 2011.

[16] Schmidt, T., Balzani, D. and Holzapfel, G.A. Statistical approach for a micromechanically based continuum description of damage evolution in soft collagenous tissues. *Comput. Meth. Appl. Mech. Eng.*, submitted.

[17] Williams, C., Liao, J., Joyce, E.M., Wang, B., Leach, J.B., Sacks, M.S. and Wong, J.Y. Altered structural and mechanical properties in decellularized rabbit carotid arteries. *Acta Biomater.*, 5:993–1005, 2009.

[18] Schröder, J. and Neff, P. Invariant formulation of hyperelastic transverse isotropy based on polyconvex free energy functions. *Int. J. Solids Struct.*, 40:401–445, 2003.

[19] Holzapfel, G.A., Gasser, T. and Ogden, R.W. A new constitutive framework for arterial wall mechanics and a comparative study of material models. *J. Elas.*, 61:1–48, 2000.

[20] Balzani, D., Neff, P., Schröder, J. and Holzapfel, G.A. A polyconvex framework for soft biological tissues. Adjustment to experimental data. *Int. J. Solids Struct.*, 43:6052–6070, 2006.